



UNIVERSITI PUTRA MALAYSIA

***ELECTROSYNTHESIS AND MODIFICATION OF TITANIA
NANOTUBES AND INCORPORATION OF MANGANESE-NICKEL
OXIDES FOR SUPERCAPACITOR APPLICATION***

MUZAKIR MUHAMMAD MUHAMMAD

FS 2021 45



**ELECTROSYNTHESIS AND MODIFICATION OF TITANIA NANOTUBES
AND INCORPORATION OF MANGANESE-NICKEL OXIDES FOR
SUPERCAPACITOR APPLICATION**

By

MUZAKIR MUHAMMAD MUHAMMAD

**Thesis Submitted to the School of Graduate Studies, Universiti Putra
Malaysia, in Fulfilment of the Requirements for Degree of Doctor of
Philosophy**

June 2021

COPYRIGHT

All material contained within the thesis, including without limitation text, logos, icons, photographs, and all other artwork, is copyright material of Universiti Putra Malaysia unless otherwise stated. Use may be made of any material contained within the thesis for non-commercial purposes from the copyright holder. Commercial use of material may only be made with the express, prior, written permission of Universiti Putra Malaysia.

Copyright © Universiti Putra Malaysia



Abstract of thesis presented to the Senate of Universiti Putra Malaysia in fulfillment of the requirement for the degree of Doctor of Philosophy.

**ELECTROSYNTHESIS AND MODIFICATION OF TITANIA NANOTUBES
AND INCORPORATION OF MANGANESE-NICKEL OXIDES FOR
SUPERCAPACITOR APPLICATION**

By

MUZAKIR MUHAMMAD MUHAMMAD

June 2021

Chairperson : Professor Zulkarnain bin Zainal, PhD
Faculty : Science

Highly ordered titania nanotubes (TNTs) as a 1D nanostructured material have received a lot of interest for supercapacitor applications due to their large surface area and relatively low cost. In this study, TNTs was synthesized by anodization in glycerol-based electrolytes. Electrochemical reduction process was used to modify the TNTs to overcome its high resistivity. The reduced titania nanotubes (R-TNTs) show improved capacitance of 2.28 mF cm^{-2} which is 7 times higher than TNTs. The R-TNTs exhibit a rectangular cyclic voltammograms and symmetrical triangular charge-discharge curves which are ideal characteristics of electric double layer capacitors (EDLCs). Furthermore, MnO_2 , NiO and binary NiMn_2O_4 were incorporated into the nanotubular structures of R-TNTs by pulse electrodeposition (PED) to enhance the capacitive performance of R-TNTs. The capacitance increased to 50.81 mF cm^{-2} , 16.57 mF cm^{-2} and 97.52 mF cm^{-2} for $\text{MnO}_2/\text{R-TNTs}$, NiO/R-TNTs and $\text{NiMn}_2\text{O}_4/\text{R-TNTs}$, respectively. All cyclic voltammograms and galvanostatic charge-discharge curves from these samples measured in 1M KCl using three electrode-configuration indicate a pseudocapacitive contribution from the deposited metal oxides. The highest capacitance obtained for the $\text{NiMn}_2\text{O}_4/\text{R-TNTs}$ composite is attributed to the synergistic effects of the MnO_2 and NiO deposited onto high conductivity R-TNTs. Physical characterization of all the synthesized samples was conducted by field emission scanning electron microscopy (FESEM), X-ray diffraction (XRD) and X-ray photoelectron spectroscopy (XPS). Higher energy and power density of 5.31 mWh cm^{-2} and $190.91 \text{ mW cm}^{-2}$ respectively were obtained for $\text{NiMn}_2\text{O}_4/\text{R-TNTs}$ asymmetric cell in two-electrode configuration.

Abstrak tesis yang dikemukakan kepada Senat Universiti Putra Malaysia
sebagai memenuhi keperluan untuk ijazah Doktor Falsafah

**ELEKTROSINTESIS DAN PENGUBAHSUAIAN TITANIA NANOTIUB DAN
PEMUATAN OKSIDA MANGAN-NIKEL UNTUK APLIKASI
SUPERKAPASITOR**

Oleh

MUZAKIR MUHAMMAD MUHAMMAD

Jun 2021

Pengerusi : Profesor Zulkarnain bin Zainal, PhD
Fakulti : Sains

Titania nanotubular yang tersusun rapi (TNTs) sebagai bahan nano berstruktur 1D telah mendapat perhatian untuk aplikasi superkapasitor kerana luas permukaannya yang besar dan memerlukan kos yang agak rendah. Dalam kajian ini, TNTs disintesis oleh anodisasi elektrolit berasaskan gliserol. Proses penurunan elektrokimia digunakan untuk mengubahsuaikan TNTs untuk mengatasi rintangan lebih tinggi. Titania nanotubular terturun (R-TNTs) menunjukkan peningkatan kapasitan 2.28 mF cm^{-2} iaitu 7 kali lebih tinggi daripada TNTs. R-TNTs menunjukkan voltametri berkisar (CV) dan galvanostat cas nyahcas (GCD) yang merupakan ciri ideal kapasitor bersifat elektrik dua lapisan (EDLCs). Selain itu, MnO_2 , NiO dan NiMn_2O_4 binari digabungkan ke dalam struktur nanotubular R-TNTs dengan pengenapanelektro denyut berbalik (PED) untuk meningkatkan prestasi kapasitif R-TNTs. Kapasitans masing-masing meningkat kepada 50.81 mF cm^{-2} , 16.57 mF cm^{-2} dan 97.52 mF cm^{-2} untuk $\text{MnO}_2/\text{R-TNT}$, NiO/RTNTs dan $\text{NiMn}_2\text{O}_4/\text{R-TNT}$. Semua CV dan keluk GCD dari sampel ini diukur dalam 1M KCl menggunakan konfigurasi tiga elektrod menunjukkan sumbangan pseudokapasitans dari oksida logam yang tersimpan. Kapasitans tertinggi yang diperoleh untuk komposit $\text{NiMn}_2\text{O}_4/\text{R-TNTs}$ dikaitkan dengan kesan sinergi MnO_2 dan NiO yang dienapkan ke R-TNTs berkonduksian tinggi. Pencirian fizikal semua sampel yang disintesis dilakukan dengan mikroskopi pengimbasan elektron pancaran medan (FESEM), analisis pembelauan sinar-X (XRD) dan spektroskopi fotoelektron sinar-X (XPS). Ketumpatan tenaga dan daya yang lebih tinggi masing-masing 5.31 mWh cm^{-2} dan $190.91 \text{ mW cm}^{-2}$ diperoleh untuk sel asimetri $\text{NiMn}_2\text{O}_4/\text{R-TNTs}$ dalam konfigurasi dua elektrod.

ACKNOWLEDGEMENTS

First of all, I thank almighty Allah for his endless blessings and strength throughout this wonderful journey. My sincere gratitude goes to my supervisor Prof. Dr. Zulkarnain Zainal for his invaluable guidance, continuous support, and encouragement throughout this project. I wish to also express my appreciations to my co-supervisors Prof. Dr. Janet Lim Hong Ngee and Associate Prof. Dr. Abdul Halim Abdullah for their useful insights, comments, and assistance. I would like to also thank Associate Prof. Dr. Tan Kar Ban for his assistance in my characterization. Sincere appreciation is extended to Dr. Mohd Haniff Wahid for the advice and encouragement. I specially acknowledged and appreciate Dr. Noor Nazihah Binti Bahrudin for her valuable suggestions and comments on my thesis.

I would like to sincerely acknowledge the Tertiary Education Trust Fund (TETFUND) and Gombe State University, Nigeria for their sponsorship and support to undertake this PhD study.

Special thanks to the staffs of microscopic units, Institute of Bioscience, Institute of Advanced Technology, UPM and MIMOS Bhd for their help in FESEM, EDX and XPS analysis. My deep appreciation to my lab mates and friends for their contributions, support, and encouragement throughout my study.

Last but not the least, my heartfelt gratitude to my mother, father, wife and children and the rest of my family for their love, prayers, encouragement, patience, and support. Thank you all.

This thesis was submitted to the Senate of Universiti Putra Malaysia and has been accepted as fulfilment of the requirement for the degree of Doctor of Philosophy. The members of the Supervisory Committee were as follows:

Zulkarnaian bin Zainal, PhD

Professor
Faculty of ChM. Science
Universiti Putra Malaysia
(Chairman)

Janet Lim Hong Ngee, PhD

Professor
Faculty of Science
Universiti Putra Malaysia
(Member)

Abdul Halim bin Abdullah, PhD

Associate Professor
Faculty of Science
Universiti Putra Malaysia
(Member)

ZALILAH MOHD SHARIFF, PhD

Professor and Dean
School of Graduate Studies
Universiti Putra Malaysia

Date: 11 November 2021

Declaration by Members of Supervisory Committee

This is to confirm that:

- the research conducted and the writing of this thesis was under our supervision;
- supervision responsibilities as stated in the Universiti Putra Malaysia (Graduate Studies) Rules 2003 (Revision 2012-2013) are adhered to.

Signature: _____
Name of Chairman
of Supervisory
Committee: Zulkarnain bin Zainal

Signature: _____
Name of Member
of Supervisory
Committee: Janet Lim Hong Ngee

Signature: _____
Name of Member
of Supervisory
Committee: Abdul Halim bin Abdullah

TABLE OF CONTENTS

	Page
ABSTRACT	i
ABSTRAK	ii
ACKNOWLEDGEMENTS	iii
APPROVAL	iv
DECLARATION	vi
LIST OF TABLES	xi
LIST OF FIGURES	xiv
LIST OF ABBREVIATIONS AND SYMBOLS	xxi
CHAPTER	
1 INTRODUCTION	1
1.1 General Introduction	1
1.2 Background of Supercapacitors	3
1.3 Brief History and Prospects of Supercapacitors	3
1.4 Problem Statement	4
1.5 Objectives of the Study	6
2 LITERATURE REVIEW	7
2.1 Principles of Energy Storage Mechanisms in Supercapacitor	7
2.1.1 Electric Double Layer Capacitors	7
2.1.2 Pseudocapacitance	9
2.2 Electrode Materials	10
2.2.1 EDLCs Materials	11
2.2.2 Pseudocapacitance Materials	11
2.3 Synthesis of Titania Nanotubes	12
2.3.1 Sol-gel Method	12
2.3.2 Atomic Layer Deposition	13
2.3.3 Hydrothermal Method	13
2.3.4 Anodic Oxidation	13
2.4 Titania Nanotubes Growth by Anodization	18
2.5 Modification of Titania Nanotubes	19
2.5.1 Electrochemical and Thermal Approaches	20
2.5.2 Metal oxides and Conducting Polymers Doping Approach	24
3 METHODOLOGY	36
3.1 Synthesis of Titania Nanotubes	36
3.1.1 Influence of Water Content	37
3.1.2 Influence of Anodization Voltage and Time	37
3.2 Modification of TNTs by Electrochemical Reduction	37
3.3 Synthesis of MnO ₂ /R-TNTs, and NiO/R-TNTs samples	37
3.3.1 Synthesis of Binary NiMn ₂ O ₄ /R-TNTs	38
3.3.2 Variation of Pulse Potentials	38
3.3.3 Variation of Duty Cycle	38

3.3.4	Variation of Deposition Time	39
3.3.5	Variation of Electrolyte Concentration	39
3.3.6	Variation of electrolyte pH	39
3.4	Characterization of the Synthesized Samples	39
3.4.1	X-ray Diffraction	40
3.4.2	Field Emission Scanning Electron Microscopy	40
3.4.3	X-ray Photoelectron Spectroscopy	40
3.5	Electrochemical Measurements	41
3.5.1	Cyclic Voltammetry	41
3.5.2	Galvanostatic Charge-Discharge	42
3.5.3	Cycle Life Test	42
3.5.4	Electrochemical Impedance Spectroscopy	43
3.5.5	Assembly of Symmetrical Cell	43
4	SYNTHESIS AND MODIFICATION OF TITANIA NANOTUBES AND THEIR ELECTROCHEMICAL PROPERTIES	45
4.1	Physico-chemical Characterization of Synthesized Titania Nanotubes	45
4.1.1	X-ray Diffraction	45
4.1.2	Field Emission Scanning Electron Microscopy	46
4.2	Electrochemical Properties of Synthesized Titania Nanotubes	51
4.3	Physico-Chemical Characterisation of Modified Titania nanotubes by Electrochemical Reduction	59
4.3.1	X-ray Diffraction	59
4.3.2	Field Emission Scanning Electron Microscopy	60
4.3.3	X-ray Photoelectron Microscopy	61
4.4	Electrochemical Properties of Modified Titania Nanotubes	62
5	PULSE ELECTRODEPOSITION OF MnO₂ ON R-TNTs AND ITS ELECTROCHEMICAL MEASUREMENTS	70
5.1	Determination of Pulse Potential Range for Electrodeposition of MnO ₂	70
5.2	Physico-chemical Characterization of synthesized MnO ₂ /R-TNTs	71
5.2.1	X-ray Diffraction	71
5.2.2	Field Emission Scanning Electron Microscopy	72
5.2.3	X-Ray Photoelectron Spectroscopy	78
5.3	Electrochemical Properties of MnO ₂ /R-TNTs	81
5.3.1	Effect of Pulse Potential	81
5.3.2	Effect of Duty Cycle	83
5.3.3	Effect of Electrolytes Concentration	85
5.3.4	Effect of Electrolyte Ph	87
5.3.5	Effect of Deposition Time	89
6	PULSE ELECTRODEPOSITION OF NiO ON R-TNTs AND ITS ELECTROCHEMICAL MEASUREMENTS	95
6.1	Determination of Pulse Potential Range for Electrodeposition of NiO	95
6.2	Physical Characterization of synthesized NiO/R-TNTs	96

6.2.1	X-ray Diffraction	96
6.2.2	Field Emission Scanning Electron Microscopy	97
6.2.3	X-Ray Photoelectron Spectroscopy	99
6.3	Electrochemical Properties of NiO/R-TNTs	101
6.3.1	Effect of Pulse Potential	101
6.3.2	Effect of Duty Cycle	103
6.3.3	Effect of Electrolytes Concentration	105
6.3.4	Effect of Electrolyte Ph	107
6.3.5	Effect of Deposition Time	109
7	PULSE ELECTRODEPOSITION OF BINARY NiMn₂O₄ ON R-TNTs AND ITS ELECTROCHEMICAL MEASUREMENTS	114
7.1	Determination of Pulse Potential Range for Electrodeposition of NiMn ₂ O ₄	114
7.2	Physico-Chemical Characterization of synthesized NiMn ₂ O ₄ /R-TNTs	115
7.2.1	X-ray Diffraction	115
7.2.2	Field Emission Scanning Electron Microscopy	116
7.2.3	X-Ray Photoelectron Spectroscopy	119
7.3	Electrochemical Properties of NiMn ₂ O ₄ /R-TNTs	120
7.3.1	Effect of Pulse Potential	121
7.3.2	Effect of Duty Cycle	123
7.3.3	Effect of Electrolytes Concentration	125
7.3.4	Effect of Electrolyte pH	127
7.3.5	Effect of Deposition Time	129
8	ASSYMBLY OF SYMMETRIC SUPERCAPACITOR CELL	135
8.1	Cycle Stability Test	135
8.2	Electrochemical Impedance Spectroscopy	138
8.3	Ragone Plots	140
9	CONCLUSION AND RECOMMENDATIONS	142
9.1	Conclusion	142
9.2	Recommendations for Future Research	144
	REFERENCES	145
	APPENDICES	161
	BIODATA OF STUDENT	175
	PUBLICATIONS	176

LIST OF TABLES

Table		Page
2.1	Comparison of the properties of EDLCs, and pseudocapacitance	10
2.2	Summary of Capacitance of Modified Anodic TNTs Electrode by Electrochemical and Thermal Approaches	23
2.3	A comparison of capacitive performance of various MnO ₂ doped TNTs and other composites materials as supercapacitor electrode	28
2.4	A comparison of capacitive performance of various NiO doped TNTs and other composites materials as supercapacitor electrode	31
2.5	A comparison of specific capacitance of various binary Ni-Mn oxides composites as supercapacitor electrodes	34
3.1	Duty cycle set-up for the overall T_{on} of 6 min	38
3.2	Pulse electrodeposition parameters for variation of electrolyte pH	39
4.1	Morphological parameters of TNTs synthesized at 25% water content for 1 h at different anodization voltage	49
4.2	Estimated Tube length of TNTs synthesized at 25% water content, 30 V at various anodization duration	51
4.3	Areal capacitance of TNTs synthesized at 20 V for 1h at different water contents, obtained from GCD at 30 V at current density of 0.02 mA/cm ²	53
4.4	Optimum conditions of synthesis of TNTs by anodization	57
5.1	Elemental analysis from EDX of MnO ₂ /R-TNTs synthesized at 10% duty cycle, 5 mM, for 6 min at different deposition potentials.	75
5.2	Elemental analysis from EDX of MnO ₂ /R-TNTs synthesized at -0.6 V, 10% duty cycle, 5 mM, at different deposition time	77
5.3	Areal capacitance of MnO ₂ /R-TNTs deposited at different pulse potential, obtained from CV at scan rate of 5 mV s ⁻¹ and GCD at current density of 0.1 mA cm ⁻²	83

5.4	Areal capacitance of MnO ₂ /R-TNTs deposited at different duty cycle, obtained from CV at scan rate of 5 mV s ⁻¹ and GCD at current density of 0.1 mA cm ⁻²	85
5.5	Areal capacitance of MnO ₂ /R-TNTs deposited at different concentrations, obtained from CV at scan rate of 5 mV s ⁻¹ and GCD at current density of 0.1 mA cm ⁻²	87
5.6	Areal capacitance of MnO ₂ /R-TNTs deposited at different pH, obtained from CV at scan rate of 5 mV s ⁻¹ and GCD at current density of 0.1 mA cm ⁻²	89
5.7	Areal capacitance of MnO ₂ /R-TNTs deposited at different deposition times, obtained from CV at scan rate of 5 mV s ⁻¹ and GCD at current density of 0.1 mA cm ⁻²	91
5.8	Optimum conditions for synthesis of MnO ₂ /R-TNTs sample	91
6.1	Areal capacitance of NiO/R-TNTs deposited at different pulse potential, obtained from CV at scan rate of 5 mV s ⁻¹ and GCD at current density of 0.1 mA cm ⁻²	103
6.2	Areal capacitance of NiO/R-TNTs deposited at different duty cycles, obtained from CV at scan rate of 5 mV s ⁻¹ and GCD at current density of 0.1 mA cm ⁻²	105
6.3	Areal capacitance of NiO/R-TNTs deposited at different concentrations, obtained from CV at scan rate of 5 mV s ⁻¹ and GCD at current density of 0.1 mA cm ⁻²	107
6.4	Areal capacitance of NiO/R-TNTs deposited at different electrolyte pH, obtained from CV at scan rate of 5 mV s ⁻¹ and GCD at current density of 0.1 mA cm ⁻²	109
6.5	Areal capacitance of NiO/R-TNTs deposited at different deposition time, obtained from CV at scan rate of 5 mV s ⁻¹ and GCD at current density of 0.1 mA cm ⁻²	111
6.6	Optimum conditions for synthesis of NiO/R-TNTs sample	111
7.1	Elemental analysis of NiMn ₂ O ₄ /R-TNTs synthesized at 1.2 V, 10% duty cycle, 1:3 Mn to Ni molar ratio at different deposition time	119
7.2	Elemental analysis of NiMn ₂ O ₄ /R-TNTs from XPS analysis.	120

7.3	Areal capacitance of NiMn ₂ O ₄ /R-TNTs deposited at different pulse potential, obtained from CV at scan rate of 5 mV s ⁻¹ and GCD at current density of 0.1 mA cm ⁻²	121
7.4	Areal capacitance of NiMn ₂ O ₄ /R-TNTs deposited at different duty cycles, obtained from CV at scan rate of 5 mV s ⁻¹ and GCD at current density of 0.1 mA/cm ²	125
7.5	Areal capacitance of NiMn ₂ O ₄ /R-TNTs deposited at different Mn to Ni molar ratio, obtained from CV at scan rate of 5 mV s ⁻¹ and GCD at current density of 0.1 mA/cm ²	127
7.6	Areal capacitance of NiMn ₂ O ₄ /R-TNTs deposited at different electrolyte pH, obtained from CV at scan rate of 5 mV s ⁻¹ and GCD at current density of 0.1 mA/cm ²	129
7.7	Areal capacitance of NiMn ₂ O ₄ /R-TNTs deposited at different deposition time, obtained from CV at scan rate of 5 mV s ⁻¹ and GCD at current density of 0.1 mA/cm ²	131
7.8	Optimum conditions for synthesis of NiMn ₂ O ₄ /R-TNTs sample	131
8.1	Cell-electrolyte resistance (R_s) and charge transfer resistance (R_{ct}) of TNTs, R-TNTs, MnO ₂ /R-TNTs, NiO/R-TNTs, and NiMn ₂ O ₄ /R-TNTs obtained from impedance analysis	140

LIST OF FIGURES

Figure		Page
1.1	Comparison of theoretical specific capacitances of TMO	2
1.2	Global supercapacitors market	4
2.1	Models of the electrical double layer at a positively charged surface: (a) the Helmholtz model, (b) the Gouy–Chapman model, and (c) the Stern model, showing the inner Helmholtz plane (IHP) distance of closest approach of specifically adsorbed ions and outer Helmholtz plane (OHP) where the diffuse layer begins; Ψ_0 and Ψ are the potentials at the electrode surface and the electrode/electrolyte interface, respectively	9
2.2	Electrochemical anodization setup	14
2.3	(a) Mechanisms of oxide formation on the metal surface, (b) different morphologies of the metal oxide- compact oxide film, disordered porous metal oxide, oriented porous oxide, and oriented nanotubular oxide (c) mechanisms of nanotubes formation	15
2.4	(a) Schematic processes during anodization, and (b) formation of TNTs	19
2.5	FESEM images of (a) R-TNTs and Mn_2O_3 deposited onto R-TNTs at different duty cycles: (b) 10%, (c) 25%, (d) 50%, (e) 75% and (f) 90% at -0.90 V (E_{on}) and 0.00 V (E_{off}) for 5 min	25
2.6	Areal capacitance of (a) $\text{Mn}_2\text{O}_3/\text{R-TNTs}$ deposited at 10% duty cycle at various current densities and (b) R-TNTs and $\text{Mn}_2\text{O}_3/\text{R-TNTs}$ synthesized at 10% duty cycle.	26
2.7	(B and B') top-view, and (C and C') cross-sectional view of FESEM images of NiO/TiO_2 by hydrothermal synthesis and electrochemical synthesis, respectively	30
3.1	Ti foil cut into desired dimensions of $1 \times 1\text{ cm}$ (1 cm extra was used as electrode holder)	36
3.2	A schematic representation of Nyquist plot	43
4.1	XRD pattern of optimized TNTs obtained at 25% water content, 30 V, for 90 min anodization voltage and time (a) as-anodized TNTs, (b) TNTs calcined at $500\text{ }^\circ\text{C}$.	46

4.2	Surface view FESEM images of TNTs synthesized in (a) 5, (b) 25, (c) 50, (d) 70, and (e) 90 v/v% water content at constant voltage of 20 V for 1h.	47
4.3	Surface view FESEM images of TNTs synthesized at 25% water content for 1 h, at (a) 10, (b) 20, (c) 30, (d) 40, and (e) 50 V.	49
4.4	Cross-sectional FESEM images of TNTs synthesized at 25% water content, 30 V for (a) 30 min, (b) 60 min, (c & d) 90 min, (e & f) 120 min at higher and lower magnification, respectively.	50
4.5	(a) Cyclic voltammograms and (b) GCD curves of TNTs synthesized at 20 V for 1 h at different water contents, collected at scan rate of 20 mV s ⁻¹ and current density of 0.02 mA cm ⁻² respectively, in 1 M KCl.	52
4.6	(a) Cyclic voltammograms and (b) GCD curves of TNTs synthesized at 25% water content for 1 h at different anodization voltage, collected at scan rate of 20 mV s ⁻¹ and current density of 0.02 mA cm ⁻² respectively, in 1 M KCl and (c) variation of areal capacitances with applied voltage.	54
4.7	(a) Cyclic voltammograms and (b) GCD curves of TNTs synthesized at 25% water content, 30 V for different anodization time, collected at scan rate of 20 mV s ⁻¹ and current density of 0.02 mA cm ⁻² respectively, in 1 M KCl and (c) variation of areal capacitances with anodization time.	56
4.8	(a) Cyclic voltammograms and (b) GCD curves of TNTs synthesized at optimum conditions, collected at different scan rate and current density respectively, in 1 M KCl and (c) areal capacitances as a function of current density.	58
4.9	XRD pattern of (a) TNTs synthesized at optimum conditions and calcined at 500 °C and (b) R-TNTs at 5 V, and 30 s reduction voltage and time.	59
4.10	Surface view FESEM images of (a) TNTs synthesized at optimum conditions, (b) R-TNTs, obtained at 5 V, and 30 s reduction voltage and time, and (c) cross-sectional view of R-TNTs.	60
4.11	Survey scan XPS spectrum of (a) TNTs synthesised at optimum conditons, and (b) R-TNTs at optimum reduction conditons.	61

4.12	Ti 2p XPS spectra (a) TNTs, (b) R-TNTs and O 1s XPS spectra (c) TNTs, (d) R-TNTs.	62
4.13	(a) Cyclic voltammograms and (b) GCD curves of R-TNTs at different reduction voltage. collected at scan rate of 200 mV s ⁻¹ and current density of 0.02 mA cm ⁻² respectively, in 1 M KCl.	63
4.14	(a) Cyclic voltammograms and (b) GCD curves of R-TNTs at different reduction time. collected at scan rate of 200 mV s ⁻¹ and current density of 0.02 mA cm ⁻² respectively, in 1 M KCl.	65
4.15	Variation of areal capacitance of R-TNTs reduced at 5 V, for 30s as a function of applied reduction (a) voltage, and (b) time.	66
4.16	Comparison of (a) Cyclic voltammograms of TNTs and R-TNTs at optimum conditions. Collected at scan rate of 200 mV s ⁻¹ and (b) GCD curves of TNTs and R-TNTs at optimum conditions recored at current density of 0.02 mA cm ⁻² , in 1 M KCl.	67
4.17	(a) Cyclic voltammograms of optimized R-TNTs at different scan rates, (b) GCD curves of optimized R-TNTs at different current densities, and (c) Variation of areal capacitance of optimized R-TNTs as a function of current density.	69
5.1	5 th Cyclic voltammogram of mixture of MnSO ₄ and Na ₂ SO ₄ at a scan rate of 20 mV s ⁻¹ .	71
5.2	XRD pattern of (a) R-TNTs, and (b) MnO ₂ /R-TNTs synthesized at optimum conditions of -0.6 V, 10% duty cycle, 5 mM, pH 6.1, for 12 min. inset figure is large image of MnO ₂ peak at 35.1° which overlap with Ti.	72
5.3	FESEM images of MnO ₂ deposited onto R-TNTs at different potentials (a) -0.6 V, (b) -0.7 V, (c) -0.8 V, and (d) -0.9 V using 10% duty cycle for 6 min.	73
5.4	Tube diameter and wall thickness of MnO ₂ / R-TNTs as a function of pulse deposition potentials.	74
5.5	EDX spectra of MnO ₂ /R-TNTs deposited at different pulse potential (a) -0.6 V, (b) -0.7 V, (c) -0.8 V, and (d) -0.9 V	74

5.6	FESEM images of MnO ₂ deposited onto R-TNTs at different deposition time (a) 3 min, (b) 6 min, (c) 9 min, and (d) 12 min, and (e) 15 min at -0.6 V using 10% duty cycle	76
5.7	Tube diameter and wall thickness of MnO ₂ /R-TNTs deposited at different at different deposition time.	76
5.8	EDX spectra of MnO ₂ /R-TNTs synthesized at -0.6 V, 10% duty cycle, 5 mM at different deposition time of (a) 3 min, (b) 6 min, (c) 9 min, and (d) 15 min.	77
5.9	XPS spectra of MnO ₂ /R-TNTs (a) survey scan, (b) Mn2p scan, and (c) O 1s scan.	78
5.10	The outputs of PED of MnO ₂ /R-TNTs for few selected cycles at different deposition time of (a) 3, (b) 6, (c) 9, (d) 12 and (e) 15 min.	80
5.11	(a) Cyclic voltammograms collected at a scan rate of 5 mV s ⁻¹ , and (b) GCD curves at 0.1 mA cm ⁻² of MnO ₂ /R-TNTs in 1 M KCl deposited at different pulse potentials using 10% duty cycle, 5 mM concentration for 6 min.	82
5.12	(a) Cyclic voltammograms collected at a scan rate of 5 mV s ⁻¹ , and (b) GCD curves at 0.1 mA cm ⁻² of MnO ₂ /R-TNTs in 1 M KCl deposited at different duty cycles using -0.6 V, 5 mM concentration for 6 min.	84
5.13	(a) Cyclic voltammograms collected at a scan rate of 5 mV s ⁻¹ , and (b) GCD curves at 0.1 mA cm ⁻² of MnO ₂ /R-TNTs in 1 M KCl deposited at different concentrations using -0.6 V, 10% duty cycle for 6 min.	86
5.14	(a) Cyclic voltammograms collected at a scan rate of 5 mV s ⁻¹ , and (b) GCD curves at 0.1 mA cm ⁻² of MnO ₂ /R-TNTs in 1 M KCl deposited at different pH using -0.6 V, 10% duty cycle, 5 mM concentrations for 6 min.	88
5.15	(a) Cyclic voltammograms collected at a scan rate of 5 mV s ⁻¹ , and (b) GCD curves at 0.1 mA cm ⁻² of MnO ₂ /R-TNTs in 1 M KCl deposited at different deposition times using -0.6 V, 10% duty cycle, 5 mM concentrations, pH 6.1.	90
5.16	(a) Cyclic voltammograms of MnO ₂ /R-TNTs deposited at optimum conditions at different scan rates in 1 M KCl, and (b) Areal capacitance as a function of scan rate.	93

5.17	(a) Galvanostatic charge discharge curves of MnO ₂ /R-TNTs deposited at optimum conditions at different current density in 1 M KCl, and (b) Areal capacitance as a function of current density.	94
6.1	Cyclic voltammogram of mixture of NiSO ₄ and Na ₂ SO ₄ at a scan rate of 20 mV s ⁻¹ .	96
6.2	XRD pattern of (a) R-TNTs, and (b) NiO/R-TNTs synthesized at optimum conditions.	97
6.3	Surface FESEM image of NiO/R-TNTs synthesized at -0.6 V, 10% duty cycle for 12 min.	98
6.4	EDS spectra of optimized NiO/R-TNTs synthesized at -0.6 V, 10% duty cycle for 12 min.	98
6.5	XPS spectra of NiO/R-TNTs (a) survey scan, (b) Ni2p scan, and (c) O 1s scan.	100
6.6	(a) Cyclic voltammograms collected at a scan rate of 5 mV s ⁻¹ , and (b) GCD curves at 0.1 mA cm ⁻² of NiO/R-TNTs in 1 M KCl deposited at different pulse potentials using 10% duty cycle, 5 mM concentration for 6 min.	102
6.7	(a) Cyclic voltammograms collected at a scan rate of 5 mV s ⁻¹ , and (b) GCD curves at 0.1 mA cm ⁻² of NiO/R-TNTs in 1 M KCl deposited at different duty cycles using -0.6 V, 5 mM concentration for 6 min.	104
6.8	(a) Cyclic voltammograms collected at a scan rate of 5 mV s ⁻¹ , and (b) GCD curves at 0.1 mA cm ⁻² of NiO/R-TNTs in 1 M KCl deposited at different concentrations using -0.6 V, 10% duty cycle for 6 min.	106
6.9	(a) Cyclic voltammograms collected at a scan rate of 5 mV s ⁻¹ , and (b) GCD curves at 0.1 mA cm ⁻² of NiO/R-TNTs in 1 M KCl deposited at different electrolyte pH using -0.6 V, 10% duty cycle and 10 mM concentration for 6 min deposition time.	108
6.10	(a) Cyclic voltammograms collected at a scan rate of 5 mV s ⁻¹ , and (b) GCD curves at 0.1 mA cm ⁻² of NiO/R-TNTs in 1 M KCl deposited at different deposition time using -0.6 V, 10% duty cycle and 10 mM concentration and pH 8.1.	110
6.11	(a) Cyclic voltammograms of NiO/R-TNTs deposited at optimum conditions at different scan rates in 1 M KCl, and (b) Areal capacitance as a function of scan rate.	112

6.12	(a) Galvanostatic charge discharge curves of NiO/R-TNTs deposited at optimum conditions at different current density in 1 M KCl, and (b) Areal capacitance as a function of current density.	113
7.1	Cyclic voltammogram of mixture of MnSO ₄ and NiSO ₄ at a scan rate of 20 mV s ⁻¹ .	115
7.2	XRD pattern of (a) R-TNTs, and (b) NiMn ₂ O ₄ /R-TNTs samples synthesized at optimum conditions. Insets Figures are larger image of NiMn ₂ O ₄ peaks at 35.4° and 62.4° which overlap with Ti.	116
7.3	Surface FESEM images of NiMn ₂ O ₄ /R-TNTs synthesized at different deposition time (a) 6 min, (b) 9 min, and (c) 12 min at optimum conditions of 1.2 V, 10% duty cycle, and 1:2 Mn to Ni molar ratio.	117
7.4	EDX spectra of NiMn ₂ O ₄ /R-TNTs synthesized at different deposition time of (a) 6 min, (b) 9 min, and (c) 12 min at optimum conditions of 1.2 V deposition potential, 10% duty cycle, and 1:2 Mn to Ni molar ratio.	118
7.5	XPS spectra of NiMn ₂ O ₄ /R-TNTs (a) survey scan, (b) Mn 2p scan, (c) Ni 2p, and (d) O 1s scan.	120
7.6	(a) Cyclic voltammograms collected at a scan rate of 5 mV s ⁻¹ , and (b) GCD curves at 0.1 mA cm ⁻² of NiMn ₂ O ₄ /R-TNTs in 1 M KCl deposited at different pulse potentials using 10% duty cycle, Mn to Ni molar ratio of 1:2, and 6 min deposition time.	122
7.7	(a) Cyclic voltammograms collected at a scan rate of 5 mV s ⁻¹ , and (b) GCD curves at 0.1 mA cm ⁻² of NiMn ₂ O ₄ /R-TNTs in 1 M KCl deposited at different duty cycles using -0.6 V, 1:2 Mn to Ni molar ration, and 6 min deposition time.	124
7.8	(a) Cyclic voltammograms collected at a scan rate of 5 mV s ⁻¹ , and (b) GCD curves at 0.1 mA cm ⁻² of NiMn ₂ O ₄ /R-TNTs in 1 M KCl deposited at different molar ratio using -0.6 V, 10% duty cycle, and 6 min deposition time.	126
7.9	(a) Cyclic voltammograms collected at a scan rate of 5 mV s ⁻¹ , and (b) GCD curves at 0.1 mA cm ⁻² of NiMn ₂ O ₄ /R-TNTs in 1 M KCl deposited at different electrolyte pH using -0.6 V, 10% duty cycle, Mn to Ni molar ratio of 1:3, and 6 min deposition time.	128

7.10	(a) Cyclic voltammograms collected at a scan rate of 5 mV s ⁻¹ , and (b) GCD curves at 0.1 mA cm ⁻² of NiMn ₂ O ₄ /R-TNTs in 1 M KCl deposited at different deposition time using -0.6 V, 10% duty cycle, Mn to Ni molar ratio of 1:3, and pH 7.5.	130
7.11	(a) Cyclic voltammograms of NiMn ₂ O ₄ /R-TNTs deposited at optimum conditions at different scan rates in 1 M KCl, and (b) Areal capacitance as a function of scan rate.	133
7.12	(a) Galvanostatic charge discharge curves of NiMn ₂ O ₄ /R-TNTs deposited at optimum conditions at different current density in 1 M KCl, and (b) Areal capacitance as a function of current density.	134
8.1	Schematic diagram for symmetric supercapacitor assembly of TNTs electrodes	135
8.2	Variation of capacitance retention of TNTs, R-TNTs, MnO ₂ /R-TNTs, NiO/R-TNTs, and NiMn ₂ O ₄ /R-TNTs samples as a function of charge discharge cycle number investigated in 1 M KCl.	137
8.3	Variation of coulombic efficiency of TNTs, R-TNTs, MnO ₂ /R-TNTs, NiO/R-TNTs, and NiMn ₂ O ₄ /R-TNTs samples as a function of charge discharge cycle number investigated in 1 M KCl.	137
8.4	Nyquist plots of (a) TNTs and R-TNTs (inset is enlarged high frequency region of the Nyquist plot), (b) MnO ₂ /R-TNTs, NiO/R-TNTs, and NiMn ₂ O ₄ /R-TNTs in 1 M KCl as a function of frequency.	139
8.5	Ragone plot for TNTs, R-TNTs, MnO ₂ /R-TNTs, NiO/R-TNTs, and NiMn ₂ O ₄ /R-TNTs symmetric supercapacitor in 1 M KCl.	141

LIST OF ABBREVIATIONS AND SYMBOLS

ALD	Atomic Layer Deposition
BTMO	Binary Transition Metal Oxides
C_A	Areal Capacitance
CV	Cyclic Voltammetry
DC	Direct Current
DI	Deionized Water
E	Energy Density
EDLC	Electric Double Layer Capacitance
EDX	Energy Dispersive X-ray Spectroscopy
EIS	Electrochemical Impedance Spectroscopy
FESEM	Field Emission Scanning Electron Microscopy
G	Glycerol
GCD	Galvanostatic charge discharge
IHP	Inner Helmholtz Plane
$Mn_2O_3/R-TNTs$	Manganese Oxide/ Reduced Titania Nanotubes
$NiMn_2O_4/R-TNTs$	Nickel Manganese Oxide/ Reduced Titania Nanotubes
$NiO/R-TNTs$	Nickel Oxide/ Reduced Titania Nanotubes
OHP	Outer Helmholtz Plane
P	Power Density
PED	Pulse Electrodeposition
R_{ct}	Charge Transfer Resistance
R_s	Cell Electrolyte Resistance
R-TNTs	Reduced Titania Nanotubes
SCs	Supercapacitors

SSC	Symmetric Supercapacitor
TEM	Transmission Electron Microscopy
TMOs	Transition Metal Oxides
TNTs	Titania Nanotubes
T_{off}	off-time
T_{on}	on-time
V_{off}	Dissolution Potential
V_{on}	Deposition Potential
XPS	X-ray Photoelectron Spectroscopy
XRD	X-ray Diffraction

CHAPTER 1

INTRODUCTION

1.1 General Introduction

Development and design of clean, renewable, and sustainable energy storage devices has increased in recent years due to increasing energy consumption, rapid depletion of fossil fuels and worsening environmental pollution (Abdah et al., 2020; Gopi et al., 2020; Wu et al., 2017). Thus, finding new, highly efficient, low cost and environmentally friendly energy storage systems is undoubtedly important considering the needs of modern technology developments in the world today (Silva et al., 2020). In this context, supercapacitors (SCs) also known as electrochemical capacitors (ECs) or ultracapacitors have gained great attention from researchers worldwide owing to their ability to bridge the performance gap between batteries and conventional capacitors in terms of high energy and power densities and long term cycling stability (Abdah et al., 2019). These advantages of SCs make them suitable for many potential applications in different industrial technology as energy storage devices.

In general, SCs are classified into two major groups based on their energy storage mechanism namely, electric double layer capacitors (EDLCs) and pseudocapacitors. In EDLCs, energy storage and release is achieved by nanoscopic charge separation at the electrode electrolyte interface which is non-faradaic and do not involve any chemical redox reaction and relatively long cycle life (Stoller & Ruoff, 2010; Vangari et al., 2013). The performance of EDLCs strongly depends on the available surface area of the electrode that is accessible to the electrolyte ions (Iro et al., 2016). On the contrary, pseudocapacitors are based on fast and reversible faradaic redox reactions occurring on or near the surface of the electrode (Samsudin et al., 2016).

In comparison, both types of SCs can store large amount of energy and release more power than the conventional capacitors and batteries, respectively with addition of rapid charge-discharge cycles and long-term cycling stability than batteries. These desirable properties make them suitable for use in various applications such as electric vehicles (EVs) or hybrid electric vehicles (HEVs), memory backup, regenerative braking in elevators, cranes and trains etc. (Afif et al., 2019).

From the material point of view, the typical materials for EDLCs are carbon-based materials with large specific surface area and high electrical conductivity such as activated carbon (Gurten Inal & Aktas, 2020), graphene (Pham et al., 2020), carbon nanotubes (CNTs) (Krajewski et al., 2019). Meanwhile, transition metal oxides (TMOs) and conducting polymers are common materials for pseudocapacitors due to their large theoretical capacitance and fast redox

kinetics (Thangappan et al., 2018). The most promising material in TMOs for pseudocapacitance is ruthenium oxide (RuO_2) but unfortunately, its high cost and toxicity make it unsuitable for large scale applications (Abdah et al., 2020). Researchers focus their attention on finding alternative materials to RuO_2 with relatively low cost and environmental compatibility TMOs such as MnO_2 (Dai et al., 2020), NiO (Endut et al., 2013b), SnO_2 (Xu et al., 2019), Fe_3O_4 (Elrouby et al., 2017), binary transition metal oxides (Tahmasebi, et al., 2016) and ternary transition metal oxides/hydroxides (Lee et al., 2020). Conducting polymers such as polyaniline, polypyrrole and polythiophene have also been used as pseudocapacitor materials (Ravit et al., 2019) or in combination with TMOs (Ishaq et al., 2019).

The theoretical capacitance of some TMOs is shown in Figure 1.1. From Figure 1.1, it can be observed that TMO have large theoretical capacitance, but in most cases, their practical capacitance value is far less than the theoretical value due to their poor electrical conductivity and densely packed structure (Zhou et al., 2016). Furthermore, the addition of binders to the TMOs which is one of the important steps commonly used for the preparation of the electrode can also inhibit their capacitive performance (Salari et al., 2018).

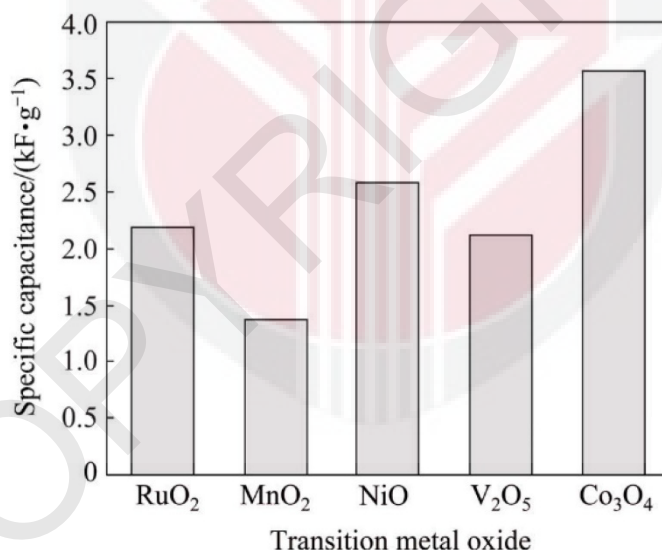


Figure 1.1: Comparison of theoretical specific capacitances of TMO
(Abdah et al., 2020)

One dimensional (1D) nanostructure materials such as tubes, wires, rods, belts have found widespread applications because of their exceptional properties in term of high surface area and electrical conductivity offering rapid electron transport and chemical reactivity. In addition, they can serve as interconnectors for fabrication of electrochemical devices such as SCs with nanoscale dimension (Hou et al., 2020). Therefore, fabrication of nanoscale TMOs on 1D

nanostructured substrate such as titania nanotubes (TNTs) will improve the electrical conductivity and pseudocapacitive performance of the TMOs.

1.2 Background of Supercapacitors

Among all the energy storage and conversion devices, supercapacitors (SCs) also known as ultracapacitors or electrochemical capacitors (ECs) have gained much attention recently due to their unique features, mainly high-power rate (typically 60-120 s discharge time), excellent reversibility (usually 90-95% or higher) and long cycling stability ($> 10^5$ cycles) (Zhang et al., 2009). They exhibit higher energy density than conventional capacitors and higher power density than batteries and fuel cells. Capacitance C , is defined as the ratio of total amount of charge (q) stored or transferred to the applied voltage (V) (Afif et al., 2019). It is an important parameter in determining the ability of the active material to store electrical charge. Other important parameters for evaluation of SCs performance includes energy density, power density and cycle life.

1.3 Brief History and Prospects of Supercapacitors

The idea of storing an electrical charge on surfaces begin in ancient times from effect associated with rubbing of amber. In the early 18th century, Leyden Jar laid down what was considered the origin of the capacitors from a vessel made up of glass with thin metallic foils serving as the electrodes and the jar as dielectric. In the 1920s, the first electrolytic capacitor comes into existence. In 1957, The first and foremost EDLCs was discovered by a group of General Electric Engineers experimenting with the activated charcoal as the capacitor plates when they observed an EDLCs effect (Iro et al., 2016; Raghavendra et al., 2020).

Later, in 1966, a group of researchers at Standard Oil company of Ohio (SOHIO) designed the modern version of the EDLCs while working on fuel cell designs using activated charcoal and then licensed it to Nippon Electric Company (NEC) which was used as backup power for maintaining computer memory (Kotz and Carlen, 2000). Nippon Electric Company (NEC), Japan and Pinnacle Research Institute (PRI), USA, named their developed capacitors as supercapacitor and ultracapacitor, respectively as the commercial names while electrochemical double layer capacitor (EDLC) is the technical name used for these devices.

Also, the global SCs market is expected to continue increasing due to wider application spectrum especially in energy harvesting, locomotives such as trains and aircraft and regenerative braking systems used in elevators and HEVs. As forecasted by IDTechEx, the global market supposed to attain US\$ 8.3 billion by 2025 at a predicted compound annual growth rate (CAGR) of 30% as illustrated in Figure 1.2 (Raghavendra et al., 2020).

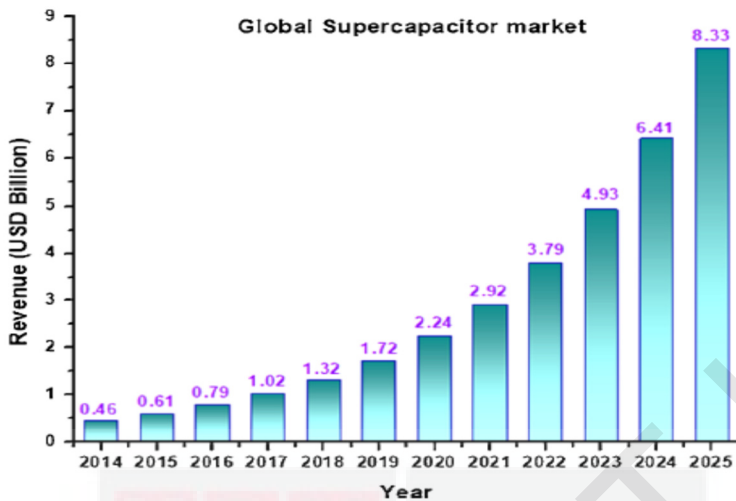


Figure 1.2: Global supercapacitors market
(Raghavendra et al., 2020)

1.4 Problem Statement

Titanium dioxide (TiO₂) or titania has been used as active electrode material in supercapacitor applications (Endut et al., 2013b; Salari, 2013) due to its unique properties such as high chemical stability, non-toxicity, low cost, developed surface area and biocompatibility (Dvorak et al., 2019; Wawrzyniak et al., 2020). However, compact titania exhibits low specific surface area and only contribute very low areal capacitance of 10-40 $\mu\text{F}/\text{cm}^2$ due to the high electrical resistance which prevents fast electron transfer (Salari, et al., 2011). Although nanocrystalline titania can increase the specific surface area of the supercapacitor electrode, the addition of binder which is an important step in electrode preparation can reduce the interconnectivity of the active titania nanoparticles with the current collector. This results in increase in resistance of the electrode apart from the additional cost.

To overcome the problem associated with compact and nanocrystalline titania, titania nanotubes (TNTs) obtained by electrochemical anodization was used due to its high accessible surface area and unique pathways resulted from the hollow structures for electron transport and short diffusion pathways for electrolytes. This fabrication route provides highly ordered; well separated nanotubes directly grown on the current collector (Ti foil) which can be used as a binder-free electrode.

It is widely reported that pristine TNTs exhibit very low capacitance less than 1 mF/cm^2 (Salari et al., 2012) which resemble conventional capacitor due to poor electrical conductivity owing to its semiconducting nature (Zhou & Zhang, 2013).

Different approaches have been adopted to improve the electrical conductivity of pristine TNTs and thus enhanced its capacitive performance through thermal treatment under reductive atmosphere (e.g. H₂, Ar, NH₃) (Lu et al., 2012; Salari, et al., 2011). However, this approach involves high temperature (above 600 °C), harsh conditions, dangerous gases which are not environmentally friendly and long-time treatment (over 10 h) (Li et al., 2015) which is not cost effective. Moreover, the highest areal capacitance (3.24 mF/cm²) (Wu et al., 2014) achieved through this approach is still small and need to be improved. In view of these disadvantages, electrochemical reduction approach carried out at ambient temperature for short duration (less than 1 minute) in simple preparation steps is considered safer, faster, and cost-effective approach for modification of TNTs.

Moreover, the electrochemically reduced TNTs (R-TNTs) showed capacitance enhancement to the value of 24.07 mF cm⁻² (Li et al., 2015) which is more than 7 times higher than the value obtained through thermal treatment. However, this capacitance value can be further increased through incorporation of TMOs into R-TNTs which can provide additional accessible surface area for the electroactive metals. To achieve this, several methods have been used such as hydrothermal, chemical bath deposition, and sono-chemical (Barai et al., 2018; Ramadoss & Kim, 2014; Zhou & Zhang, 2014a). However, these approaches involve long preparation time, elaborate procedures, high temperature, and environmentally unfriendly chemicals.

Attempts have been also made to use various electrodeposition modes such as potentiostatic or galvanostatic (Huang et al., 2015) as they are more facile, simple, and cost effective methods compared to solvothermal approach. However, the use of these electrodeposition modes leads to the formation of larger particles of the active TMOs due to the overlapping of diffusion zones which agglomerate and cover the nanotubes openings. This leads to a decrease in surface area of R-TNTs and hinders the smooth diffusion of electrolyte ions through the nanotubes.

To overcome this problem, pulse electrodeposition (PED) was adopted in this study which involves two-series of potential pulses in which one pulse consists of applying a deposition potential known as on-time followed by another potential at zero current referred to as off-time. This leads to the deposition of the metal particles uniformly distributed on R-TNTs to form a compact crystalline structure. This approach allows possibility of achieving controllable size of deposits, homogeneous distribution and suitable thickness of the active metals which is critical for the maximum performance of the electrode in SCs application.

As substitute to highly cost and toxic RuO₂, in this study, manganese oxide (MnO₂) and nickel oxide (NiO) was each incorporated into the nanotubular structure of R-TNTs by PED due to their low cost, low toxicity, redox characteristics and high theoretical capacitance (Chime et al., 2020; Kate et al., 2018) even though less than that of Co₃O₄ as shown in Figure 1.1. Nevertheless,

Co_3O_4 behaves as battery-type electrode material as its cycling stability and rate capability are affected by low electrical conductivity (An et al., 2019). Next, the binary MnO_2/NiO was also deposited into the R-TNTs to observe their synergistic effect on the improvement of capacitive performance of the SCs electrode.

1.5 Objectives of the Study

The overall objective of this study is to synthesize highly ordered TNTs as binder-free SCs electrode and enhance the capacitance through electrochemical reduction and incorporation of binary transition metal oxides. To achieve this, several objectives are outline as follows:

1. To synthesize and optimized
 - i. highly ordered titania nanotubes (TNTs) by electrochemical anodization in glycerol-based electrolyte.
 - ii. reduced titania nanotubes (R-TNTs) by electrochemical treatment of TNTs.
 - iii. $\text{MnO}_2/\text{R-TNTs}$, $\text{NiO}/\text{R-TNTs}$ and binary $\text{NiMn}_2\text{O}_4/\text{R-TNTs}$ via pulse electrodeposition (PED) method.
2. To characterize the physical and chemical properties of the TNTs, R-TNTs, $\text{MnO}_2/\text{R-TNTs}$, $\text{NiO}/\text{R-TNTs}$ and $\text{NiMn}_2\text{O}_4/\text{R-TNTs}$ using XRD, FESEM, EDX and XPS techniques.
3. To evaluate the electrochemical performance of TNTs, R-TNTs, $\text{MnO}_2/\text{R-TNTs}$, $\text{NiO}/\text{R-TNTs}$ and $\text{NiMn}_2\text{O}_4/\text{R-TNTs}$ as supercapacitor electrode.

REFERENCES

- Abbasi, N., Moradi, M., Hajati, S., Kiani, M. A., & Toth, J. (2017). In-situ growth of ultrathin Ni₆MnO₈ nanosheets on nickel foam as a binder-free positive electrode for asymmetric supercapacitor: Effects of alkaline aqueous and redox additive electrolytes. *Journal of Molecular Liquids*, 244, 269–278.
- Adelkhani, H., & Ghaemi, M. (2010). Characterization of manganese dioxide electrodeposited by pulse and direct current for electrochemical capacitor. *Journal of Alloys and Compounds*, 493(1–2), 175–178.
- Aff, A., Rahman, S. M., Tasfiah Azad, A., Zaini, J., Islan, M. A., & Azad, A. K. (2019). Advanced materials and technologies for hybrid supercapacitors for energy storage – A review. *Journal of Energy Storage*, 25(April), 100852.
- Aida, T., Yamada, K., & Morita, M. (2006). *An Advanced Hybrid Electrochemical Capacitor That Uses a Wide Potential Range at the Positive Electrode*. 534–536.
- Ain, N., Amirul, M., Mohd, A., Hawa, N., Azman, N., & Sulaiman, Y. (2020). Polyaniline and manganese oxide decorated on carbon nano fibers as a superior electrode material for supercapacitor. *Journal of Electroanalytical Chemistry*, 867, 114188.
- An, C., Zhang, Y., Guo, H., & Wang, Y. (2019). Metal oxide-based supercapacitors: progress and perspectives. *Nanoscale Advances*, 1(12), 4644–4658.
- Arsent, M. Y., Koval, N. Y., Shmigel, A. V, Tikhonov, P. A., & Kalinina, M. V. (2017). *NiMn₂O₄ Spinel as a Material for Supercapacitors with a PseudoCapacity Effect*. July, 2–6.
- Ban, F. Y., Majid, S. R., Huang, N. M., & Lim, H. N. (2012). Graphene oxide and its electrochemical performance. *International Journal of Electrochemical Science*, 7(5), 4345–4351.
- Baptista, J. M., Sagu, J. S., KG, U. W., & Lobato, K. (2019). State-of-the-art materials for high power and high energy supercapacitors: Performance metrics and obstacles for the transition from lab to industrial scale – A critical approach. *Chemical Engineering Journal*, 374(February), 1153–1179.
- Barai, H. R., Banerjee, A. N., Bai, F., & Joo, S. W. (2018). Surface modification of titania nanotube arrays with crystalline manganese-oxide nanostructures and fabrication of hybrid electrochemical electrode for high-performance supercapacitors. *Journal of Industrial and Engineering Chemistry*, 62, 409–417.

- Berger, S., Tsuchiya, H., & Schmuki, P. (2008). Transition from Nanopores to Nanotubes: Self-Ordered Anodic Oxide Structures on Titanium-Aluminides Self-ordering effects in anodic oxides on refractory metals are observed in two distinct morphologies : (i) highly ordered parallelly aligned porous oxid. *Chemistry of Materials*, 20(10), 3245–3247.
- Beyazay, T., Eylül Sarac Oztuna, F., & Unal, U. (2019). Self-Standing Reduced Graphene Oxide Papers Electrodeposited with Manganese Oxide Nanostructures as Electrodes for Electrochemical Capacitors. *Electrochimica Acta*, 296, 916–924.
- Burke, A. (2007). R&D considerations for the performance and application of electrochemical capacitors. *Electrochimica Acta*, 53(3 SPEC. ISS.), 1083–1091.
- Chang, K., & Hu, C. (2006). *Hydrothermal synthesis of binary Ru – Ti oxides with excellent performances for supercapacitors*. 52, 1749–1757.
- Chen, Y. S., & Hu, C. C. (2003). Capacitive characteristics of binary manganese-nickel oxides prepared by anodic deposition. *Electrochemical and Solid-State Letters*, 6(10).
- Cheshideh, H., & Nasirpouri, F. (2017). Cyclic voltammetry deposition of nickel nanoparticles on TiO₂ nanotubes and their enhanced properties for electro-oxidation of methanol. *Journal of Electroanalytical Chemistry*, 797(November 2016), 121–133.
- Chime, U. K., Nkele, A. C., Ezugwu, S., Nwanya, A. C., Shinde, N. M., Kebede, M., Ejikeme, P. M., Maaza, M., & Ezema, F. I. (2020). Recent progress in nickel oxide-based electrodes for high-performance supercapacitors. *Current Opinion in Electrochemistry*, 21, 175–181.
- Chua, C. W., Zainal, Z., Lim, H. N., & Chang, S. K. (2018). Effect of electrolytes on the electrochemical performance of nickel cobaltite–titania nanotubes composites as supercapacitive materials. *Journal of Materials Science: Materials in Electronics*, 29(17), 14445–14454.
- Clement Raj, C., & Prasanth, R. (2018). Review—advent of TiO₂ nanotubes as supercapacitor electrode. In *Journal of the Electrochemical Society* (Vol. 165, Issue 9, pp. E345–E358). Electrochemical Society Inc.
- Conway, B. E. (1991). Transition from “supercapacitor” to “battery” behavior in electrochemical energy storage. *Proceedings of the International Power Sources Symposium*, 138(6), 319–327.
- Da Silva, L. M., Cesar, R., Moreira, C. M. R., Santos, J. H. M., De Souza, L. G., Pires, B. M., Vicentini, R., Nunes, W., & Zanin, H. (2020). Reviewing the fundamentals of supercapacitors and the difficulties involving the analysis of the electrochemical findings obtained for porous electrode materials. *Energy Storage Materials*, 27(August 2019), 555–590.

- Dai, X., Zhang, M., Li, J., & Yang, D. (2020). Effects of electrodeposition time on a manganese dioxide supercapacitor. *RSC Advances*, 10(27), 15860–15869.
- Daniel Nixon, P., & Joseph Kennady, C. (2019). Electrodeposition of manganese-nickel oxide films for supercapacitor applications. *Voprosy Khimii i Khimicheskoi Tekhnologii*, 2019(6), 144–148.
- Di, J., Fu, X., Zheng, H., & Jia, Y. (2015). H–TiO₂/C/MnO₂ nanocomposite materials for high-performance supercapacitors. *Journal of Nanoparticle Research*, 17(6).
- Du, H., Xie, Y., Xia, C., Wang, W., Tian, F., & Zhou, Y. (2014). Preparation of a flexible polypyrrole nanoarray and its capacitive performance. *Materials Letters*, 132, 417–420.
- Dvorak, F., Zazpe, R., Krbal, M., Sopha, H., Prikryl, J., Ng, S., Hromadko, L., Bures, F., & Macak, J. M. (2019). One-dimensional anodic TiO₂ nanotubes coated by atomic layer deposition: Towards advanced applications. *Applied Materials Today*, 14, 1–20.
- El-kady, M. F. (2012). *Laser Scribing of High-Performance and Flexible Graphene-Based Electrochemical Capacitors* Laser Scribing of High-Performance and Flexible Graphene-Based Electrochemical Capacitors. March.
- Elrouby, M., Abdel-Mawgoud, A. M., & El-Rahman, R. A. (2017). Synthesis of iron oxides nanoparticles with very high saturation magnetization from TEA-Fe(III) complex via electrochemical deposition for supercapacitor applications. *Journal of Molecular Structure*, 1147, 84–95.
- Endut, Z., Hamdi, M., & Basirun, W. J. (2013). Supercapacitance of bamboo-type anodic titania nanotube arrays. *Surface and Coatings Technology*, 215, 75–78.
- Endut, Zulkarnain, Hamdi, M., & Basirun, W. J. (2013a). An investigation on formation and electrochemical capacitance of anodized titania nanotubes. *Applied Surface Science*, 280, 962–966.
- Endut, Zulkarnain, Hamdi, M., & Basirun, W. J. (2013b). Optimization and functionalization of anodized titania nanotubes for redox supercapacitor. *Thin Solid Films*, 549, 306–312.
- Environ, E. (2011). *Environmental Science PAPER A high-performance asymmetric supercapacitor fabricated with graphene-based electrodes* f. 4009–4015.
- Faid, A. Y., & Ismail, H. (2019). Ternary mixed nickel cobalt iron oxide nanorods as a high-performance asymmetric supercapacitor electrode. *Materials Today Energy*, 13, 285–292.

- Fang, B., & Binder, L. (2007). Enhanced surface hydrophobisation for improved performance of carbon aerogel electrochemical capacitor. *Electrochimica Acta*, 52(24), 6916–6921.
- Fu, Y., & Mo, A. (2018). *A Review on the Electrochemically Self-organized Titania Nanotube Arrays: Synthesis, Modifications, and Biomedical Applications*.
- Ge, M. Z., Cao, C. Y., Huang, J. Y., Li, S. H., Zhang, S. N., Deng, S., Li, Q. S., Zhang, K. Q., & Lai, Y. K. (2016). Synthesis, modification, and photo/photoelectrocatalytic degradation applications of TiO₂ nanotube arrays: A review. *Nanotechnology Reviews*, 5(1), 75–112.
- Ghalmi, Y., Habelhames, F., Sayah, A., Bahloul, A., Nessark, B., Shalabi, M., & Nunzi, J. M. (2019). Capacitance performance of NiO thin films synthesized by direct and pulse potentiostatic methods. *Ionics*, 25(12), 6025–6033.
- Ghicov, A., & Schmuki, P. (2009). Self-ordering electrochemistry: A review on growth and functionality of TiO₂ nanotubes and other self-aligned MO_x structures. *Chemical Communications*, 20, 2791–2808.
- Giorgi, L., Salernitano, E., Dikonimos Makris, T., Giorgi, R., Leoni, E., Grilli, M. L., & Lisi, N. (2016). Titania nanotubes self-assembled by electrochemical anodization: Semiconducting and electrochemical properties. *Thin Solid Films*, 601, 28–34.
- Guo, M., Balamurugan, J., Kim, N. H., & Lee, J. H. (2018). High-energy solid-state asymmetric supercapacitor based on nickel vanadium oxide/NG and iron vanadium oxide/NG electrodes. *Applied Catalysis B: Environmental*, 239(January), 290–299.
- Gurten Inal, I. I., & Aktas, Z. (2020). Enhancing the performance of activated carbon based scalable supercapacitors by heat treatment. *Applied Surface Science*, 514(August 2019), 145895.
- Hakamada, M., Moriguchi, A., & Mabuchi, M. (2014). Fabrication of carbon nanotube/NiO_x(OH)_y nanocomposite by pulsed electrodeposition for supercapacitor applications. *Journal of Power Sources*, 245, 324–330.
- He, M., Li, J., Xu, W., Dong, Z., Wu, Y., & Lv, L. (2019). Carbon Nanotubes/MnO₂ Composite Fabricated via Laser Welding and Electrodeposition as Flexible Electrode for Supercapacitors. *Nano*, 14(6), 1–8.
- He, M., Zheng, Y., & Du, Q. (2013). Electrodeposition of polypyrrole/MnO₂ nanocomposite on graphite felt as free-standing electrode for supercapacitors. *Nano*, 8(2), 1–7.

- Hou, H., Shao, G., Yang, W., & Wong, W. Y. (2020). One-dimensional mesoporous inorganic nanostructures and their applications in energy, sensor, catalysis and adsorption. *Progress in Materials Science*, 113(September 2019), 100671.
- Huang, Y. G., Zhang, X. H., Chen, X. B., Wang, H. Q., Chen, J. R., Zhong, X. X., & Li, Q. Y. (2015). Electrochemical properties of MnO₂-deposited TiO₂ nanotube arrays 3D composite electrode for supercapacitors. *International Journal of Hydrogen Energy*, 40(41), 14331–14337.
- Imran Sohail, Z. H., & Ahmad Nawaz Khan, K. Y. (2017). d M us. *Mater. Res. Express*, 1–16.
- Indira, K., Mudali, U. K., Nishimura, T., & Rajendran, N. (2015). A Review on TiO₂ Nanotubes: Influence of Anodization Parameters, Formation Mechanism, Properties, Corrosion Behavior, and Biomedical Applications. *Journal of Bio- and Tribo-Corrosion*, 1(4), 1–22.
- Iro, Z. S., Subramani, C., & Dash, S. S. (2016). A brief review on electrode materials for supercapacitor. *International Journal of Electrochemical Science*, 11(12), 10628–10643.
- Ishaq, S., Moussa, M., Kanwal, F., Ehsan, M., Saleem, M., Van, T. N., & Losic, D. (2019). Facile synthesis of ternary graphene nanocomposites with doped metal oxide and conductive polymers as electrode materials for high performance supercapacitors. *Scientific Reports*, 9(1), 1–11.
- Jaafar, H. I., Alsammerraei, A. M. A., & Hamdan, H. H. (2012). *Study of the effect of NH₄F concentration on the structure of electrochemically prepared TiO₂ nanotubes* TiO₂ (NH₄F). 53(2), 827–831.
- Kate, R. S., Khalate, S. A., & Deokate, R. J. (2018). Overview of nanostructured metal oxides and pure nickel oxide (NiO) electrodes for supercapacitors: A review. *Journal of Alloys and Compounds*, 734, 89–111.
- Kazemi, S. H., & Abdollahi Aghdam, S. (2019). High-Performance Asymmetric Supercapacitor Based on Ternary MnO₂-Polyaniline-Reduced Graphene Oxide Quantum Dots Nanocomposite Electrode. *Journal of Electronic Materials*.
- Kelly-Holmes, H. (2016). Advertising as multilingual communication. *Advertising as Multilingual Communication*, 45, 1–206.
- Khaja Hussain, S., Nagaraju, G., Chandra Sekhar, S., & Yu, J. S. (2019). Morphological synergistic behavior on electrochemical performance of battery-type spinel nickel manganese oxides for aqueous hybrid supercapacitors. *Journal of Power Sources*, 439(September), 227088.

- Khudhair, D., Bhatti, A., Li, Y., Hamedani, H. A., Garmestani, H., Hodgson, P., & Nahavandi, S. (2016). Anodization parameters influencing the morphology and electrical properties of TiO₂ nanotubes for living cell interfacing and investigations. *Materials Science and Engineering C*, *59*, 1125–1142.
- Kim, B. C., Ko, J. M., & Wallace, G. G. (2008). A novel capacitor material based on Nafion-doped polypyrrole. *Journal of Power Sources*, *177*(2), 665–668.
- Kim, H. Y., Shin, J., Jang, I. C., & Ju, Y. W. (2019). Hydrothermal synthesis of three-dimensional perovskite NiMnO₃oxide and application in supercapacitor electrode. *Energies*, *13*(1).
- Kim, T., Ramadoss, A., Saravanakumar, B., Veerasubramani, G. K., & Kim, S. J. (2016). Synthesis and characterization of NiCo₂O₄ nanoplates as efficient electrode materials for electrochemical supercapacitors. *Applied Surface Science*, *370*, 452–458.
- Kim, Y., Jung, J., Kim, S., & Chae, W. S. (2013). Cyclic voltammetric and chronoamperometric deposition of CdS. *Materials Transactions*, *54*(8), 1467–1472.
- Krajewski, M., Liao, P. Y., Michalska, M., Tokarczyk, M., & Lin, J. Y. (2019). Hybrid electrode composed of multiwall carbon nanotubes decorated with magnetite nanoparticles for aqueous supercapacitors. *Journal of Energy Storage*, *26*(September), 101020.
- Krishnamoorthy, S., Tyagi, A., & Gupta, R. K. (2018). Carbon Nanostructures from Biomass Waste for Supercapacitor Applications. *Nanomaterials*, *June*, 261–282.
- Krishnan, S. G., Archana, P. S., Vidyadharan, B., Misnon, I. I., Vijayan, B. L., Nair, V. M., Gupta, A., & Jose, R. (2016). Modification of capacitive charge storage of TiO₂ with nickel doping. *Journal of Alloys and Compounds*, *684*, 328–334.
- Kuanxin, H., Xiaogang, Z., & Juan, L. (2006). Preparation and electrochemical capacitance of Me double hydroxides (Me = Co and Ni)/TiO₂ nanotube composites electrode. *Electrochimica Acta*, *51*(7), 1289–1292.
- Kulandaivalu, S., & Sulaiman, Y. (2019). Recent advances in layer-by-layer assembled conducting polymer based composites for supercapacitors. *Energies*, *12*(11).
- Lee, H. M., Lee, K., & Kim, C. K. (2014). Electrodeposition of manganese-nickel oxide films on a graphite sheet for electrochemical capacitor applications. *Materials*, *7*(1), 265–274.
- Lee, K., Mazare, A., & Schmuki, P. (2014). One-dimensional titanium dioxide nanomaterials: Nanotubes. *Chemical Reviews*, *114*(19), 9385–9454.

- Lee, S. C., Liu, S., Shinde, P. A., Chung, K. Y., & Chan Jun, S. (2020). A systematic approach to achieve high energy density hybrid supercapacitors based on Ni–Co–Fe hydroxide. *Electrochimica Acta*, 353, 136578.
- Li, J., Wang, X., Yu, X., Ma, C., & Zhao, J. (2016). Fabrication of MnO₂/TiO₂ nanotube arrays composite films through a one-step redox precipitation method. *International Journal of Hydrogen Energy*, 41(47), 22162–22170.
- Li, L., Zhang, X., Wu, G., Peng, X., Huo, K., & Chu, P. K. (2015). Supercapacitor Electrodes Based on Hierarchical Mesoporous MnOx/Nitrided TiO₂ Nanorod Arrays on Carbon Fiber Paper. *Advanced Materials Interfaces*, 2(6), 1–10.
- Li, Zhen, Ding, Y., Kang, W., Li, C., Lin, D., Wang, X., Chen, Z., Wu, M., & Pan, D. (2015). Reduction Mechanism and Capacitive Properties of Highly Electrochemically Reduced TiO₂ Nanotube Arrays. *Electrochimica Acta*, 161, 40–47.
- Li, Zhongwei, Wang, X., Wang, X., Xiao, T., Zhang, L., Lv, P., & Zhao, J. (2018). Preparation and properties of MnO₂–TiO₂ nanotube array composite electrodes using titanium foam as the current collector. *International Journal of Hydrogen Energy*, 43(18), 8859–8867.
- Lim, Y. C., Zainal, Z., Hussein, M. Z., & Tan, W. T. (2012). Effect of water content on structural and photoelectrochemical properties of titania nanotube synthesized in fluoride ethylene glycol electrolyte. *Advanced Materials Research*, 501(April), 204–208.
- Lim, Y. C., Zainal, Z., Tan, W. T., & Hussein, M. Z. (2012). Anodization parameters influencing the growth of titania nanotubes and their photoelectrochemical response. *International Journal of Photoenergy*, 2012(January).
- Lim, Y., Zainal, Z., & Hussein, M. Z. (2012). *Effect of Water Content on Structural and Photoelectrochemical Properties of Titania Nanotube Synthesized in Fluoride Ethylene Glycol Electrolyte Effect of Water Content on Structural and Photoelectrochemical Properties of Titania Nanotube Synthesized in*. May 2014.
- Liu, R.S., Zhang, L., Sun, X., Liu, H., & Zhang, J. (2011). *Lithium Ion Rechargeable Batteries High Energy Density Lithium Batteries Nanostructured Materials in Electrochemistry Electrocatalysis of Direct Methanol Fuel Cells Advanced Lithium-Ion Batteries*.
- Liu, H., Liang, Z., Liu, S., Zhang, L., Xia, H., & Xie, W. (2020). Nickel manganese hydroxides with thin-layer nanosheets and multivalences for high-performance supercapacitor. *Results in Physics*, 16(December 2019), 102831.

- Liu, J., Li, J., Dai, M., Hu, Y., Cui, J., Wang, Y., Tan, H. H., & Wu, Y. (2018). Photo-assisted synthesis of coaxial-structured polypyrrole/electrochemically hydrogenated TiO₂ nanotube arrays as a high performance supercapacitor electrode. *RSC Advances*, 8(24), 13393–13400.
- Liu, Q., Zhang, H., Xie, J., Liu, X., & Lu, X. (2020). Recent progress and challenges of carbon materials for Zn-ion hybrid supercapacitors. *Carbon Energy*, June, 1–19.
- Liu, X. Y., Zhou, M., Chen, C., & Zhang, Y. X. (2017). Electrochemical capacitor performance of TiO₂ nanostructures and porous MnO₂ composite supported on carbon fiber paper. *Ceramics International*, 43(13), 10595–10600.
- Lo, A. Y., Saravanan, L., Tseng, C. M., Wang, F. K., & Huang, J. T. (2020). Effect of Composition Ratios on the Performance of Graphene/Carbon Nanotube/Manganese Oxide Composites toward Supercapacitor Applications. *ACS Omega*, 5(1), 578–587.
- Long, X., Wang, H., Wang, C., Cao, X., & Li, X. (2019). Enhancement of azo dye degradation and power generation in a photoelectrocatalytic microbial fuel cell by simple cathodic reduction on titania nanotube arrays electrode. *Journal of Power Sources*, 415(April 2018), 145–153.
- Low, W. H., Khiew, P. S., Lim, S. S., Siong, C. W., & Ezeigwe, E. R. (2019). Recent development of mixed transition metal oxide and graphene/mixed transition metal oxide based hybrid nanostructures for advanced supercapacitors. *Journal of Alloys and Compounds*, 775, 1324–1356.
- Lu, X., Wang, G., Zhai, T., Yu, M., & Zhou, L. (2012). Hydrogenated TiO₂ nanotube arrays as high-rate anodes for lithium-ion microbatteries. *Nano Lett.*, 12, 1690–1696.
- Macak, J. M., Gong, B. G., Hueppe, M., & Schmuki, P. (2007). Filling of TiO₂ nanotubes by self-doping and electrodeposition. *Advanced Materials*, 19(19), 3027–3031.
- Macak, J. M., & Schmuki, P. (2006). Anodic growth of self-organized anodic TiO₂ nanotubes in viscous electrolytes. *Electrochimica Acta*, 52(3), 1258–1264.
- Marichi, R. B., Sahu, V., & Sharma, R. K. (n.d.). *Efficient, Sustainable, and Clean Energy Storage in Supercapacitors Using Biomass-Derived Carbon Materials*. 1–26.
- Masuda, H., Masuda, H., Fukuda, K., & Fukuda, K. (1995). Ordered Metal Nanohole Arrays Made. *Science*, 268(June), 1466–1468.
- Miller, J. R., & Simon, P. (2012). *Electrochemical Capacitors for Energy Management*. 651(2008).

- Mirzaee, M., & Dehghanian, C. (2018). Pulsed electrodeposition of reduced graphene oxide on Ni–NiO foam electrode for high-performance supercapacitor. *International Journal of Hydrogen Energy*, 43(27), 12233–12250.
- Mohd Abdah, M. A. A., Azman, N. H. N., Kulandaivalu, S., Abdul Rahman, N., Abdullah, A. H., & Sulaiman, Y. (2019). Potentiostatic deposition of poly(3, 4-ethylenedioxythiophene) and manganese oxide on porous functionalised carbon fibers as an advanced electrode for asymmetric supercapacitor. *Journal of Power Sources*, 444(June), 227324.
- Mohd Abdah, M. A. A., Azman, N. H. N., Kulandaivalu, S., & Sulaiman, Y. (2020). Review of the use of transition-metal-oxide and conducting polymer-based fibres for high-performance supercapacitors. *Materials and Design*, 186, 108199.
- Mohd Abdah, M. A. A., Zubair, N. A., Azman, N. H. N., & Sulaiman, Y. (2017). Fabrication of PEDOT coated PVA-GO nanofiber for supercapacitor. *Materials Chemistry and Physics*, 192, 161–169.
- Momeni, M. M., & Ahadzadeh, I. (2015). Fabrication of tungsten decorated titania nanotube arrays as electrode materials for supercapacitor applications. *International Journal of Hydrogen Energy*, 40(29), 8769–8777.
- Moses Ezhil Raj, A., Victoria, S. G., Jothy, V. B., Ravidhas, C., Wollschläger, J., Suendorf, M., Neumann, M., Jayachandran, M., & Sanjeeviraja, C. (2010). XRD and XPS characterization of mixed valence Mn₃O₄ hausmannite thin films prepared by chemical spray pyrolysis technique. *Applied Surface Science*, 256(9), 2920–2926.
- Mujawar, S. H., Ambade, S. B., Battumur, T., Ambade, R. B., & Lee, S. H. (2011). Electropolymerization of polyaniline on titanium oxide nanotubes for supercapacitor application. *Electrochimica Acta*, 56(12), 4462–4466.
- Muralee Gopi, C. V. V., Vinodh, R., Sambasivam, S., Obaidat, I. M., & Kim, H. J. (2020). Recent progress of advanced energy storage materials for flexible and wearable supercapacitor: From design and development to applications. *Journal of Energy Storage*, 27(September 2019), 101035.
- Muzaffar, A., Ahamed, M. B., Deshmukh, K., & Thirumalai, J. (2019). A review on recent advances in hybrid supercapacitors: Design, fabrication and applications. *Renewable and Sustainable Energy Reviews*, 101(July 2018), 123–145.
- Nycz, M., & Arkusz, K. (2019). *Influence of the Silver Nanoparticles (AgNPs) Formation Conditions onto Titanium Dioxide (TiO₂) Nanotubes Based Electrodes on Their Impedimetric Response.*

- Pan, D., Huang, H., Wang, X., Wang, L., Liao, H., Li, Z., & Wu, M. (2014). C-axis preferentially oriented and fully activated TiO₂ nanotube arrays for lithium ion batteries and supercapacitors. *Journal of Materials Chemistry A*, 2(29), 11454–11464.
- Pham, M. H., Khazaeli, A., Godbille-Cardona, G., Truica-Marasescu, F., Peppley, B., & Barz, D. P. J. (2020). Printing of graphene supercapacitors with enhanced capacitances induced by a leavening agent. *Journal of Energy Storage*, 28(October 2019), 101210.
- Potphode, D., Sayed, M. S., Lama Tamang, T., & Shim, J. J. (2019). High-performance binder-free flower-like (Ni_{0.66}Co_{0.3}Mn_{0.04})₂(OH)₂(CO₃) array synthesized using ascorbic acid for supercapacitor applications. *Chemical Engineering Journal*, 378(January), 122129.
- Raghavendra, K. V. G., Vinoth, R., Zeb, K., Muralee Gopi, C. V. V., Sambasivam, S., Kummara, M. R., Obaidat, I. M., & Kim, H. J. (2020). An intuitive review of supercapacitors with recent progress and novel device applications. *Journal of Energy Storage*, 31(June), 101652.
- Raj, C. C., & Prasanth, R. (2018). Review—Advent of TiO₂ Nanotubes as Supercapacitor Electrode. *Journal of The Electrochemical Society*, 165(9), E345–E358.
- Raj, C. C., Sundheep, R., & Prasanth, R. (2015). Enhancement of electrochemical capacitance by tailoring the geometry of TiO₂ nanotube electrodes. *Electrochimica Acta*, 176, 1214–1220.
- Ramadoss, A., & Kim, S. J. (2014). Hierarchically structured TiO₂@MnO₂ nanowall arrays as potential electrode material for high-performance supercapacitors. *International Journal of Hydrogen Energy*, 39(23), 12201–12212.
- Ravit, R., Abdullah, J., Ahmad, I., & Sulaiman, Y. (2019). Electrochemical performance of poly(3, 4-ethylenedioxythiophene)/nanocrystalline cellulose (PEDOT/NCC) film for supercapacitor. *Carbohydrate Polymers*, 203(June 2018), 128–138.
- Regonini, D., Bowen, C. R., Jaroenworarluck, A., & Stevens, R. (2013). A review of growth mechanism, structure and crystallinity of anodized TiO₂ nanotubes. *Materials Science and Engineering R: Reports*, 74(12), 377–406.
- Regonini, D., & Clemens, F. J. (2015). Anodized TiO₂ nanotubes: Effect of anodizing time on film length, morphology and photoelectrochemical properties. *Materials Letters*, 142, 97–101.
- Roy, P., Berger, S., & Schmuki, P. (2011a). TiO₂ nanotubes: Synthesis and applications. *Angewandte Chemie - International Edition*, 50(13), 2904–2939.

- Roy, P., Berger, S., & Schmuki, P. (2011b). TiO₂ nanotubes: Synthesis and applications. *Angewandte Chemie - International Edition*, 50(13), 2904–2939.
- Salari, M. (2013). *Functionalization of nanostructured titania (TiO₂) as electrode materials for supercapacitors*. <http://ro.uow.edu.au/theses/3824>
- Salari, M., Aboutalebi, S. H., Chidembo, A. T., Innis, P. C., Konstantinov, K., Liu, H. K., & Schmuki, P. (2014). Design of self-assembled TiO₂ architectures: Towards hybrid nanotubular interfaces. *Physica Status Solidi (A) Applications and Materials Science*, 211(4), 938–945.
- Salari, M., Aboutalebi, S. H., Chidembo, A. T., Nevirkovets, I. P., Konstantinov, K., & Liu, H. K. (2012). Enhancement of the electrochemical capacitance of TiO₂ nanotube arrays through controlled phase transformation of anatase to rutile. *Physical Chemistry Chemical Physics*, 14(14), 4770–4779.
- Salari, M., Aboutalebi, S. H., Ekladios, I., Jalili, R., Konstantinov, K., Liu, H. K., & Grinstaff, M. W. (2018). Tubular TiO₂ Nanostructures: Toward Safer Microsupercapacitors. *Advanced Materials Technologies*, 3(2), 1–7.
- Salari, M., Aboutalebi, S. H., Konstantinov, K., & Liu, H. K. (2011). A highly ordered titania nanotube array as a supercapacitor electrode. *Physical Chemistry Chemical Physics*, 13(11), 5038–5041.
- Salari, M., Konstantinov, K., & Liu, H. K. (2011). Enhancement of the capacitance in TiO₂ nanotubes through controlled introduction of oxygen vacancies. *Journal of Materials Chemistry*, 21(13), 5128–5133.
- Samsudin, N. A., Zainal, Z., Lim, H.-N., Sulaiman, Y., & Chang, S.-K. (2016). Titania Nanotubes Synthesised via the Electrochemical Anodisation Method: Synthesis and Supercapacitor Applications. *Pjsrr*, 2(1), 107–128.
- Samsudin, N. A., Zainal, Z., Lim, H. N., Sulaiman, Y., Chang, S. K., Lim, Y. C., Ayal, A. K., & Mohd Amin, W. N. (2018). Capacitive performance of vertically aligned reduced titania nanotubes coated with Mn₂O₃ by reverse pulse electrodeposition. *RSC Advances*, 8(41), 23040–23047.
- Samsudin, N. A., Zainal, Z., Lim, H. N., Sulaiman, Y., Chang, S. K., Lim, Y. C., & Mohd Amin, W. N. (2018). Enhancement of Capacitive Performance in Titania Nanotubes Modified by an Electrochemical Reduction Method. *Journal of Nanomaterials*, 2018.
- Shan, Q., Huo, W., Shen, M., Jing, C., Peng, Y., Pu, H., & Zhang, Y. (2020). Melamine sponge derived porous carbon monoliths with NiMn oxides for high performance supercapacitor. *Chinese Chemical Letters*, 2019, 2–5.

- Shen, Y., Dastafkan, K., Sun, Q., Wang, L., Ma, Y., Wang, Z., & Zhao, C. (2019). Improved electrochemical performance of nickel-cobalt hydroxides by electrodeposition of interlayered reduced graphene oxide. *International Journal of Hydrogen Energy*, 44(7), 3658–3667.
- Song, Y., Li, Y., Guo, J., Gao, Z., & Li, Y. (2015). Facile method to synthesize a carbon layer embedded into titanium dioxide nanotubes with metal oxide decoration for electrochemical. *Journal of Materials Chemistry A: Materials for Energy and Sustainability*, 00, 1–6.
- Sreekantan, S., Saharudin, K. A., Lockman, Z., & Tzu, T. W. (2010). Fast-rate formation of TiO₂ nanotube arrays in an organic bath and their applications in photocatalysis. *Nanotechnology*, 21(36).
- Stoller, M. D., & Ruoff, R. S. (2010). *Best practice methods for determining an electrode material 's performance for ultracapacitors*. 1294–1301.
- Sun, S., Liao, X., Yin, G., Yao, Y., Huang, Z., & Pu, X. (2016). Enhanced electrochemical performance of TiO₂ nanotube array electrodes by controlling the introduction of substoichiometric titanium oxides. *Journal of Alloys and Compounds*, 680, 538–543.
- Syed Zainol Abidin, S. N. J., Mamat, M. S., Rasyid, S. A., Zainal, Z., & Sulaiman, Y. (2018). Electropolymerization of poly(3,4-ethylenedioxythiophene) onto polyvinyl alcohol-graphene quantum dot-cobalt oxide nanofiber composite for high-performance supercapacitor. *Electrochimica Acta*, 261, 548–556.
- Tahmasebi, M. H., Raeissi, K., Golozar, M. A., Vicenzo, A., Hashempour, M., & Bestetti, M. (2016). Tailoring the pseudocapacitive behavior of electrochemically deposited manganese-nickel oxide films. *Electrochimica Acta*, 190, 636–647.
- Tahmasebi, M. H., Vicenzo, A., Hashempour, M., Bestetti, M., Golozar, M. A., & Raeissi, K. (2016). Nanosized Mn-Ni oxide thin films via anodic electrodeposition: A study of the correlations between morphology, structure and capacitive behaviour. *Electrochimica Acta*, 206, 143–154.
- Tang, X., Zhang, B., Lui, Y. H., & Hu, S. (2019). Ni-Mn bimetallic oxide nanosheets as high-performance electrode materials for asymmetric supercapacitors. *Journal of Energy Storage*, 25(May), 100897.
- Thangappan, R., Arivanandhan, M., Dhinesh Kumar, R., & Jayavel, R. (2018). Facile synthesis of RuO₂ nanoparticles anchored on graphene nanosheets for high performance composite electrode for supercapacitor applications. *Journal of Physics and Chemistry of Solids*, 121(January), 339–349.
- Tholkappian, R., Naveen, A. N., Vishista, K., & Hamed, F. (2018). Investigation on the electrochemical performance of hausmannite Mn₃O₄ nanoparticles by ultrasonic irradiation assisted co-precipitation method for

- supercapacitor electrodes . *Journal of Taibah University for Science*, 12(5), 669–677.
- Tian, M., Wu, J., Li, R., Chen, Y., & Long, D. (2019). Fabricating a high-energy-density supercapacitor with asymmetric aqueous redox additive electrolytes and free-standing activated-carbon-felt electrodes. *Chemical Engineering Journal*, 363(November 2018), 183–191.
- Tran, C. C. H., Santos-Peña, J., & Damas, C. (2020). Electrodeposited manganese oxide supercapacitor microelectrodes with enhanced performance in neutral aqueous electrolyte. *Electrochimica Acta*, 335, 1–10.
- Tran, V. M., Ha, A. T., & Le, M. L. P. (2014). Capacitance behavior of nanostructured ϵ -MnO₂/C composite electrode using different carbons matrix. *Advances in Natural Sciences: Nanoscience and Nanotechnology*, 5(2).
- Tran, M. Van, Ha, A. T., & Le, P. M. L. (2015). Nanoflake manganese oxide and nickel-manganese oxide synthesized by electrodeposition for electrochemical capacitor. *Journal of Nanomaterials*, 2015.
- Vangari, M., Pryor, T., & Jiang, L. (2013). Supercapacitors: Review of Materials and Fabrication Methods. *Journal of Energy Engineering*, 139(2), 72–79.
- Vivekchand, S. R. C., Rout, C. S., Subrahmanyam, K. S., Govindaraj, A., & Rao, C. N. R. (2008). *Graphene-based electrochemical supercapacitors*. 120(1), 9–13.
- Wang, D., Li, Y., Wang, Q., & Wang, T. (2012). Facile synthesis of porous Mn₃O₄ nanocrystal-graphene nanocomposites for electrochemical supercapacitors. *European Journal of Inorganic Chemistry*, 4, 628–635.
- Wang, F., Wang, C., Zhao, Y., Liu, Z., Chang, Z., Fu, L., Zhu, Y., Wu, Y., & Zhao, D. (2016). A Quasi-Solid-State Li-Ion Capacitor Based on Porous TiO₂Hollow Microspheres Wrapped with Graphene Nanosheets. *Small*, 12(45), 6207–6213.
- Wang, F., Wu, X., Yuan, X., Liu, Z., Zhang, Y., Fu, L., Zhu, Y., Zhou, Q., Wu, Y., & Huang, W. (2017). Latest advances in supercapacitors: From new electrode materials to novel device designs. *Chemical Society Reviews*, 46(22), 6816–6854.
- Wang, J.-W., Chen, Y., & Chen, B.-Z. (2015). A Synthesis Method of MnO₂/Activated Carbon Composite for Electrochemical Supercapacitors . *Journal of The Electrochemical Society*, 162(8), A1654–A1661.
- Wawrzyniak, J., Grochowska, K., Karczewski, J., Kupracz, P., Ryl, J., Dołęga, A., & Siuzdak, K. (2020). The geometry of free-standing titania nanotubes as a critical factor controlling their optical and photoelectrochemical

- performance. *Surface and Coatings Technology*, 389(February), 125628.
- Wu, B., Ma, H., Pan, Z., Wang, J., Qu, W., & Wang, B. (2014). Drying and quality characteristics and models of carrot slices under catalytic infrared heating. *International Agricultural Engineering Journal*, 23(2), 70–79.
- Wu, H., Li, D., Zhu, X., Yang, C., Liu, D., Chen, X., Song, Y., & Lu, L. (2014). High-performance and renewable supercapacitors based on TiO₂ nanotube array electrodes treated by an electrochemical doping approach. *Electrochimica Acta*, 116, 129–136.
- Wu, H., Xu, C., Xu, J., Lu, L., Fan, Z., Chen, X., Song, Y., & Li, D. (2013). Enhanced supercapacitance in anodic TiO₂ nanotube films by hydrogen plasma treatment. *Nanotechnology*, 24(45).
- Wu, Z., Li, L., Yan, J. M., & Zhang, X. B. (2017). Materials Design and System Construction for Conventional and New-Concept Supercapacitors. *Advanced Science*, 4(6).
- Xiao, F., & Xu, Y. (2015). *Pulse Electrodeposition of Manganese Oxide for High-Rate Capability Supercapacitors*. August 2012.
- Xie, Y., Huang, C., Zhou, L., Liu, Y., & Huang, H. (2009). Supercapacitor application of nickel oxide-titania nanocomposites. *Composites Science and Technology*, 69(13), 2108–2114.
- Xie, Y., Zhou, L., Huang, C., Huang, H., & Lu, J. (2008). Fabrication of nickel oxide-embedded titania nanotube array for redox capacitance application. *Electrochimica Acta*, 53(10), 3643–3649.
- Xie, Z. B., & Blackwood, D. J. (2010). Effects of anodization parameters on the formation of titania nanotubes in ethylene glycol. *Electrochimica Acta*, 56(2), 905–912.
- Xu, M. W., Bao, S. J., & Li, H. L. (2007). Synthesis and characterization of mesoporous nickel oxide for electrochemical capacitor. *Journal of Solid State Electrochemistry*, 11(3), 372–377.
- Xu, Y., Wang, L., Zhou, Y., Guo, J., Zhang, S., & Lu, Y. (2019). Synthesis of heterostructure SnO₂/graphitic carbon nitride composite for high-performance electrochemical supercapacitor. *Journal of Electroanalytical Chemistry*, 852(August), 113507.
- Ying Chin, L., Zainal, Z., Khusaimi, Z., & Ismail, S. S. (2016). Electrochemical Synthesis of Ordered Titania Nanotubes in Mixture of Ethylene Glycol and Glycerol Electrolyte. *Malaysian Journal of Analytical Science*, 20(2), 373–381.

- Yu, C., Wang, Y., Zhang, J., Shu, X., Cui, J., Qin, Y., Zheng, H., Liu, J., Zhang, Y., & Wu, Y. (2016). Integration of mesoporous nickel cobalt oxide nanosheets with ultrathin layer carbon wrapped TiO₂ nanotube arrays for high-performance supercapacitors. *New Journal of Chemistry*, 40(8), 6881–6889.
- Yunyun, F., Xu, L., Wankun, Z., Yuxuan, Z., Yunhan, Y., Honglin, Q., Xuetao, X., & Fan, W. (2015). Spinel CoMn₂O₄ nanosheet arrays grown on nickel foam for high-performance supercapacitor electrode. *Applied Surface Science*, 357, 2013–2021.
- Zhang, C., Xing, J., Fan, H., Zhang, W., Liao, M., & Song, Y. (2017). Enlarged capacitance of TiO₂ nanotube array electrodes treated by water soaking. *Journal of Materials Science*, 52(6), 3146–3152.
- Zhang, L., & Zhao, X. S. (2009). Carbon-based materials as supercapacitor electrodes. *Chemical Society Reviews*, 38(9), 2520–2531.
- Zhang, W., Liu, Y., Song, Z., Zhuang, C., & Wei, A. (2021). The storage mechanism difference between amorphous and anatase as supercapacitors. *Green Energy and Environment*.
- Zhang, Y., Feng, H., Wu, X., Wang, L., Zhang, A., Xia, T., Dong, H., Li, X., & Zhang, L. (2009). Progress of electrochemical capacitor electrode materials: A review. *International Journal of Hydrogen Energy*, 34(11), 4889–4899.
- Zhou, H., & Zhang, Y. (2013). Enhancing the capacitance of TiO₂ nanotube arrays by a facile cathodic reduction process. *Journal of Power Sources*, 239, 128–131.
- Zhou, H., & Zhang, Y. (2014a). Enhanced electrochemical performance of manganese dioxide spheres deposited on a titanium dioxide nanotube arrays substrate. *Journal of Power Sources*, 272, 866–879.
- Zhou, H., & Zhang, Y. (2014b). Electrochemically Self-Doped TiO₂ Nanotube Arrays for Supercapacitors. *The Journal of Physical Chemistry C*, 118(11), 5626–5636.
- Zhou, H., Zou, X., & Zhang, Y. (2016). Fabrication of TiO₂@MnO₂ nanotube arrays by pulsed electrodeposition and their application for high-performance supercapacitors. *Electrochimica Acta*, 192, 259–267.
- Zhu, Y., Murali, S., Stoller, M. D., Ganesh, K. J., Cai, W., Ferreira, P. J., Pirkle, A., Wallace, R. M., Cychosz, K. A., Thommes, M., Su, D., Stach, E. A., & Ruoff, R. S. (2011). *Carbon-Based Supercapacitors*. 332(June), 1537–1542.

Zuniga, L., Gonzalez, G., Chavez, R. O., Myers, J. C., Lodge, T. P., & Alcoutlabi, M. (2019). *applied sciences* Centrifugally Spun α -Fe₂O₃ / TiO₂ / Carbon Composite Fibers as Anode Materials for Lithium-Ion Batteries.

Zuo, W., Xie, C., Xu, P., Li, Y., & Liu, J. (2017). A Novel Phase-Transformation Activation Process toward Ni–Mn–O Nanoprism Arrays for 2.4 V Ultrahigh-Voltage Aqueous Supercapacitors. *Advanced Materials*, 29(36), 1–9.

Zwilling, V., Aucouturier, M., & Darque-Ceretti, E. (1999). Anodic oxidation of titanium and TA6V alloy in chromic media. An electrochemical approach. *Electrochimica Acta*, 45(6), 921–929.

